# LOAD BEARING CHARACTERISTICS OF BORED PRECAST PRESTRESSED NODULAR PILES

**Yujiro Tanaka, Japan Pile Corporation, 36-2 Nihonbashi Hakozakicho, Chuo-ku, Tokyo, Japan, +81(0)3 5843 4196, yujiro_tanaka@japanpile.co.jp**
**Yusuke Homma, Japan Pile Corporation, 36-2 Nihonbashi Hakozakicho, Chuo-ku, Tokyo, Japan, +81(0)3 5843 4196, yusuke_honma@japanpile.co.jp**
**Kentaro Oko, ASIA PILE HOLDINGS CORPORATION, 36-2 Nihonbashi Hakozakicho, Chuo-ku, Tokyo, Japan, +81(0)3 5843 4173, kentaro_oko@asiapile-hd.com**

## ABSTRACT

Precast nodular piles, used in Japan for almost a century, are high-strength concrete spun piles with fixed-interval nodules. In the early days these piles were driven with a mound of crushed stone around the pile such that the crushed stone space, between nodules around the shaft as the pile penetrated into the ground. The installation method shifted to bored precast methods after 1970 due to regulations restricting noise pollution from impact driving. Bored precast piling involves placing piles in drilled holes, grouting with cement grout that enhances shaft friction. Recently, nodular piles are also used as bearing resistance piles. A base-enlarged pre-boring method, with an enlarged base at the pile toe, increases bearing resistance capacity. Combined with base enlargement, bored precast piles provide high axial load resistance for buildings. This paper explores the history, development, load transfer analysis, and design practice of bored prestressed high-strength concrete (PHC) nodular piles in Japan.

**Keywords: Nodular Pile, Bearing Capacity, Settlement, Loading Tests, Load Transfer Analysis.**

## INTRODUCTION

In 1923, Shojiro Takechi developed the nodular pile in Osaka, Japan. Initially developed as a 350 mm (1.15 ft) square pile, this evolved to hexagonal and heptagonal sections before the current, circular spun precast piles with nodules at every 1000 mm (3.28 ft) spacing. In general, use of precast nodular piles in Japan went through various changes in shape and installation methods over the past 80 years. With the availability of larger machinery, lager diameter nodular piles have been developed, and are considered well suited to provide higher friction resistance to support low to mid-rise structures.

## TRANSITION OF NODULAR PILE CONSTRUCTION METHODS

Around the 1930s, manual drop hammers were used to drive nodular piles with a pile of crushed rock around the pile such that the space between nodules got packed with crushed rock as it penetrated into the ground (Photo 1). By the 1960s, diesel/hydraulic hammers replaced drop hammers, the crushed rock packing approach continued as a means of soil improvement and providing drainage for excess porewater pressure through the crushed rock to serve as liquefaction mitigation. From 1960 to 2000, regulations on noise and vibration became stricter, and alternatives to impact driving for installation of piles were developed. One of the recent installation methods as an alternative to impact driving is the Geo Mixing

 

Takechi Original Pile (GMTOP) method (2000) that installs piles in cement-mixed soil holes. Another method known as the Hyper Mega (HM) method (2006), combines the MEGA Takechi Original Pile (MEGATOP) method (2003) with an enlarged base. The HM method allows 1200 mm (3.94 ft) nodule diameter nodular pile and straight shaft connections, enhancing end bearing resistance as well as the shaft friction (Fig. 1). In 2024, the HM method was used in over 4000 projects in Japan (Photo 2).

**Photo 1. Nodular pile installation using a drop hammer in the 1930s**

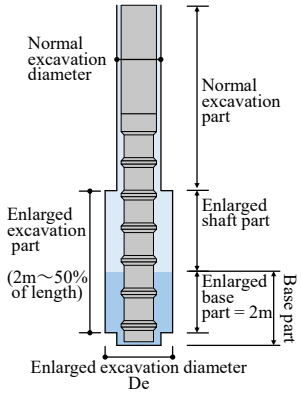


**Fig. 1. Image of Pile material and Excavation of the HM method**

**Photo 2. Nodular pile installation using the HM method**

## OVERVIEW OF THE HM METHOD

### *Applicable piles*

The HM method is applicable to various pile types, including nodular piles with a maximum node diameter of 1200 mm (3.94 ft), and straight piles like PHC, PRC, SC, and steel pipe piles, also up to 1200 mm (3.94 ft) in diameter, which can be spliced with nodular piles. These piles can be combined to suit specific design conditions. Figure 2. illustrates 1000-800 mm nodular piles (nodule diameter-shaft diameter). Enhanced horizontal and axial bearing capacity can be achieved by using an enlarged upper section, joining straight piles larger than the lower nodular pile. Piles with concrete strengths of 85, 105, and 123 N/mm² are utilized.

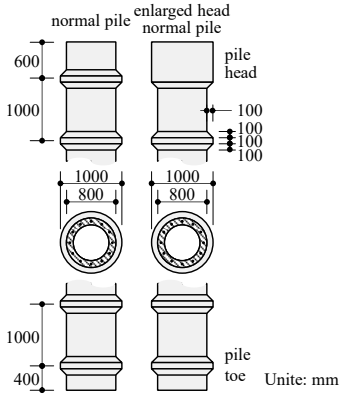


**Fig. 2. Configuration of a 1000-800 mm Nodular Pile with Enlarged Head**

 

### *Ground conditions and installation depth*

The ground to which the HM method can be applied is sandy soil, gravelly soil, and clay (including silty soil) near the pile tip, and sandy soil (including gravelly soil) and clay around the pile tip. The current maximum depth of installation is 68.5 m. In ground with liquefaction potential, a separate study is required.

### *Overview of construction procedures*

An overview of the installation procedure for the HM method is illustrated in Fig. 3. There are two types of auger heads used for bottom expansion: a mechanical type that expands cutting blades by rotating in the opposite direction and a hydraulic type that expands the cutting blades hydraulically. If the standard excavation diameter (diameter at the nodule + 50 mm) is $D_s$, and the enlarged excavation diameter is $D_e$, then the enlargement factor $\omega$ is defined as $\omega = D_e/D_s$. Work monitoring is extremely important to ensure the quality of the pile at the base enlarged pre-boring and grouting method. The key points especially are checks to confirm that the expanded blade has correctly expanded and the grout has been properly pumped. These critical items are measured and monitored by devices integrated with the construction machinery.

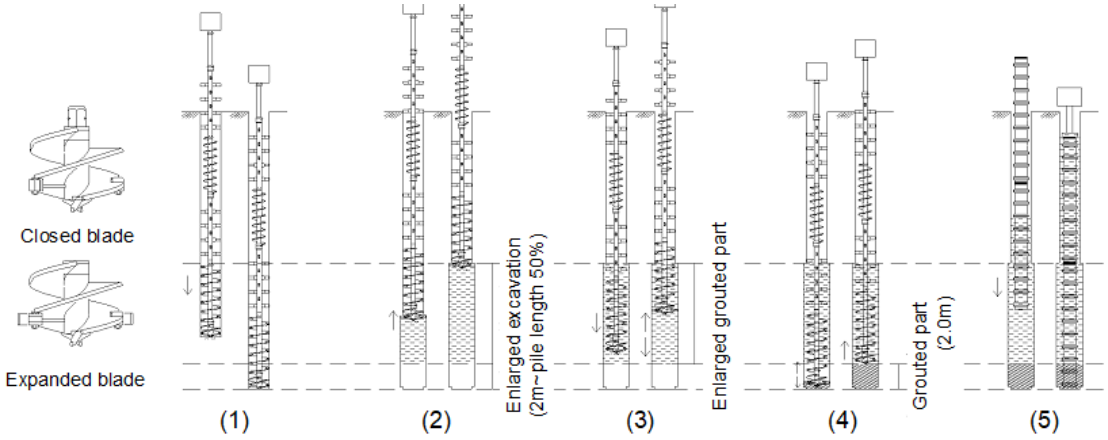


**Fig. 3. Installation sequence**

## AXIAL BEARING CAPACITY

### *Bearing resistance*

As shown in Fig. 4, the end bearing capacity $P_p$ is evaluated as the axial resistance at a position 2000 mm (6.56 ft) above the pile toe in this HM method. This evaluation position of 2000 mm above the pile toe is set to broadly consider the influence of the ground near the pile tip. For this reason, the “bearing capacity” includes the shaft friction of the 2000 mm grouted base in addition to the load bearing capacity at the bottom face of the grouted base. As the two components are not evaluated separately in the conventional design methods, these components have remained unclear in terms of the bearing capacity mechanism.

 

End bearing capacity $P_p$ in the HM method is the sum of the resistance $P_{pp}$ at the pile toe (bottom) face and the shaft friction of the grouted base $P_{pf}$ above the bottom. For $P_{pp}$, the axial force at the lowermost node position (about 350 mm above the pile toe face) is used.

To derive the equations for the bearing capacity of piles installed by the HM method, the diameter of the grout base should be considered to vary in the range of 1 to 2 times that of the standard excavation diameter (in the upper part). This range is selected based on the constructability considerations. The conventional $\alpha$ is expressed by equation [1], and the factor $a$, $b$, $c$ are determined from the data of loading tests.

$$\alpha = \alpha_p + \alpha_f = a\omega^b + c\omega \quad [1]$$

Where $\alpha_p$ = Bearing capacity factor due to load bearing capacity at the pile toe face (lowermost node bottom face); $\alpha_f$ = Bearing capacity factor due to shaft friction resistance of grouted base; $\omega$ = Enlargement ratio = $D_e$ / ($D_o$ + 0.05); $D_e$= Enlarged excavation diameter (grouted base diameter) (m); $D_o$ = Nodal diameter at the grouted base position (m)

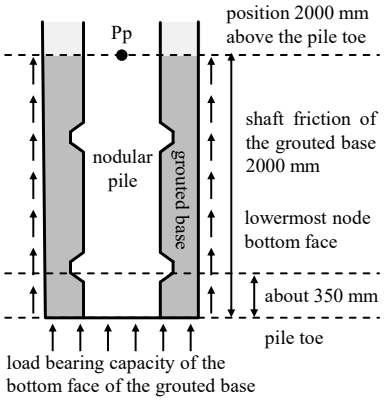


**Fig. 4. Evaluation position of pile bearing resistance capacity $P_p$**

Detailed analysis process is omitted. On the basis of the above analysis from load test results with a strain gauge, the equations of α for sandy/gravelly and clayey soils (including silty soils) are given by equations [2] and [3] respectively.

$$\alpha = 240\omega^{1.5} + 90\omega \quad [2]$$

$$\alpha = 210\omega^{1.25} + 90\omega \quad [3]$$

When $\omega$ = 2.0, the value of $\alpha$ for sandy/gravelly soil is 858 (kN/m$^2$) and for clayey soil it is 679 (kN/m$^2$). Figure 5 shows the relationship of $\alpha$ with $\omega$ compared with load test data for sandy and gravelly soil. The values in the data for both types of soil exceed those obtained from the equations.

 

***Shaft friction resistance***

Empirical equations for estimating the shaft friction resistance are derived using the friction resistance $f_s$ and $f_c$, determined from the results of loading tests. The calculation equations are as shown in [4] to [7].

$$P_{fs} = f_s L_s D\pi \quad [4]$$

$$f_s = \beta N_s \quad [5]$$

$$P_{fc} = f_c L_c D\pi \quad [6]$$

$$f_c = \gamma q_u \quad [7]$$

Where $P_{fs}$ = Shaft friction resistance of sandy soil (kN); $f_s$ = Shaft friction in sandy soil (kN/m$^2$); $L_s$ = segment length of pile in contact with sandy soil (m); $D$ = Pile diameter in meter (nodule diameter of nodular pile); $\beta$ = Shaft friction resistance factor of sandy soil; $N_s$ = Average $N$-value ($N$60) of sandy soil; $P_{fc}$ = Shaft friction resistance of clayey soil (kN); $f_c$ = Shaft friction in clayey soil (kN/m$^2$); $L_c$ = segment length of pile in contact with clayey soil (m); $\gamma$ = Shaft friction resistance factor of clayey soil (kN); $q_u$ = Measured unconfined compression strength (kN/m$^2$). Values of shaft friction resistance at ultimate load bearing capacity from equations are compared with the loading test data.

In the case of nodular piles, the occurrence of the slip surface between the pile shaft and the cement grout cannot be considered owing to the bearing resistance at nodules and their effect of integrating the pile with the cement grout. Moreover, the occurrence of the slip surface between the cement grout and the soil is observed during loading tests. Accordingly, the shaft friction resistance of nodular pile is decided by the frictional resistance between the cement grout and the soil, and is considered to be proportional to the outer diameter (excavation diameter) of the cement grout. Thus, the shaft friction stress of a nodular pile was estimated using the excavation diameter (taken as $\omega D_o$) and not the nodal diameter $D_o$.

Figure 6 shows the $f_s$ - $N_s$ relationship of sandy soil around the pile. These data were obtained from various ground conditions across Japan. Since the equation for (mean - 1.06$\sigma$) is $f_s/\omega = 30.3 + 5.50\ N_s$, the relatioship for $\beta$ is expressed by equation [8]. Fig. 7 also shows the $f_c$ - $q_u$ relationship for clayey soils. Since the equation for (mean - 1.06$\sigma$) is $f_c/\omega = 23.12 + 0.510\ q_u$, the relationship for $\gamma$ is expressed by equation [9]. The friction resistance of a Straight pile is considered that there is a case where the slip occurs between the cement grout and the pile body. This phenomenon has been confirmed in loading tests. Thus, the data is estimated by the pile diameter (not by the excavation diameter).

 

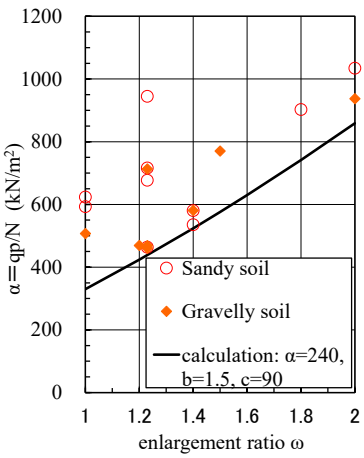


**Fig. 5. *α-ω* relationship (sandy and gravelly soil)**

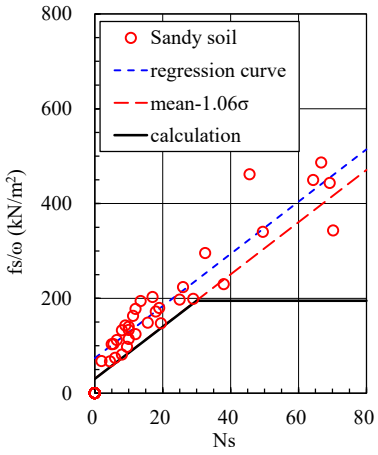


**Fig. 6. $f_s$-$N_s$ relationship (nodular pile; sandy soil)**

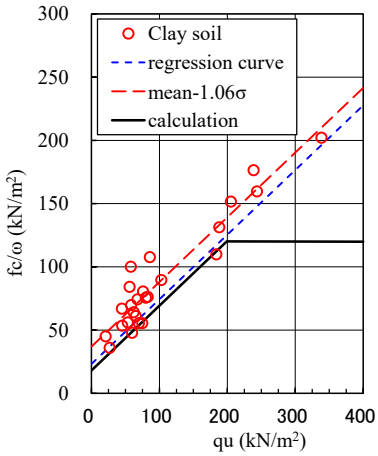


**Fig. 7. $f_c$-$q_u$ relationship (nodular pile; clayey soil)**

$$\beta\overline{N_s} = (30 + 5.5\overline{N_s})\omega \quad [8]$$

$$\gamma\overline{q_u} = (20 + 0.5\overline{q_u})\omega \quad [9]$$

## COMPARISON OF BEARING CAPACITY CHARACTERISTICS

### *Outline of comparison conditions*

The ultimate bearing capacity (measured value) obtained from the loading test results of the HM method is compared with the calculated value. Fig. 8 and Table 1 show the conditions of the ground and pile specifications used for the comparison. These ground conditions and pile specifications are selected from the results of loading tests on the piles installed by the HM method. The pile tip ground conditions are sand (tip N-value 13.6), gravel (tip N-value 33.3), and clay (tip N-value 10.0). The *N*-value is one of the indices representing ground strength, obtained through a ground investigation called the Standard Penetration Test. The Standard Penetration Test, along with the Cone Penetration Test, is widely used in Japan as part of geotechnical exploration. The conditions of the pile specifications are: pile lengths of 26 to 32 m, nodal piles with diameters 500-400 mm to 800-600 mm, and expansion ratios of 1.80 to 2.00.

 

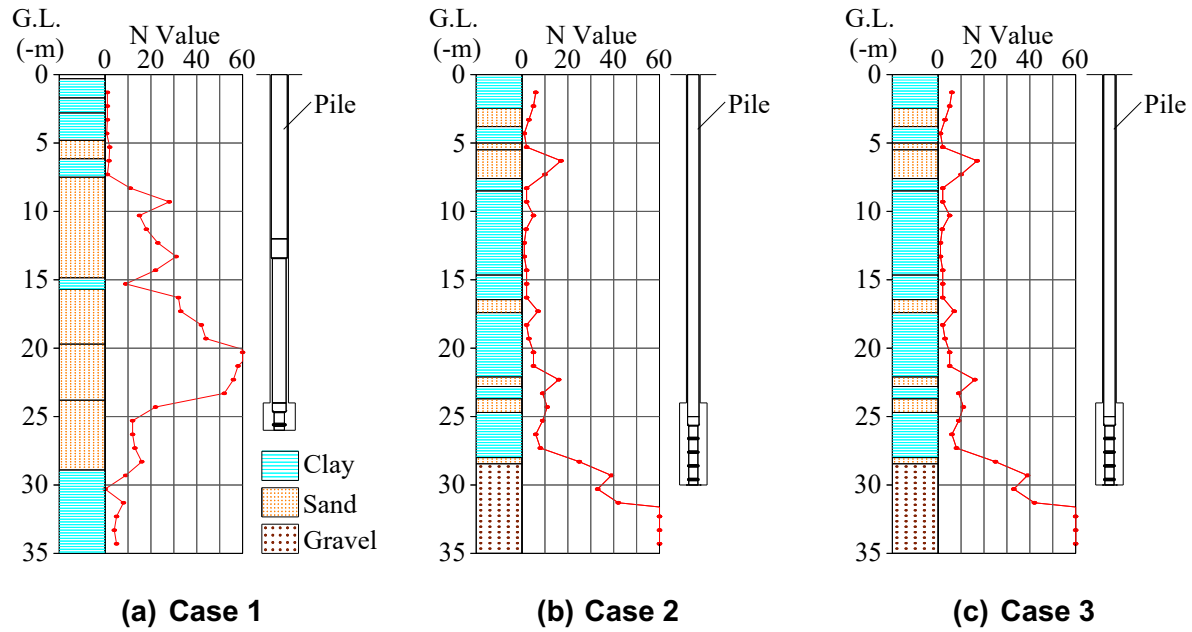


**Fig. 8. Soil and pile condition for calculation case study**

**Table 1. Soil and pile condition for calculation case study**

| Test Case | Case 1 | Case 2 | Case 3 |
|---|---|---|---|
| Soil at the pile tip | sand | gravel | clay |
| Nodular pile (nodule-shaft diameter in mm) | 600-450 | 500-400 | 800-600 |
| Overall pile length (m) | 26 | 30 | 32 |
| Enlargement ratio | 1.80 | 2.00 | 1.80 |

***Comparison results***

Table 2 shows the results of the comparison between the measured and calculated values of the ultimate bearing capacity. The ratio of measured to calculated values are in the range of 1.13 to 1.63. It was confirmed that the measured values were higher or well above the calculated values. As shown in Figs. 5-7, the parameters α, β, and γ are set on the conservative side, which results in the measured values higher than the calculated values.

**Table 2. Comparison of ultimate bearing capacity**

| Test Case | Case 1 | Case 2 | Case 3 |
|---|---|---|---|
| Measured Value from load test (kN) | 14,400 | 9,800 | 18,600 |
| Calculated Value from equation (kN) | 12,700 | 6,900 | 11,400 |
| Measured / Calculated | 1.13 | 1.42 | 1.63 |

 

## COMPARISON OF LOAD-SETTLEMENT CHARACTERISTICS

### *Verification summary*

The load-settlement relationship at the pile head and axial force distribution obtained from the loading test results of the HM method are compared with the analytical values. The ground conditions and pile specifications used in the comparison are the same as Fig. 8 and Table 1 above. The calculation method of the analytical values is described in the next section.

### *Analysis model overview*

The analytical values are obtained using a load transfer analysis. Load transfer analysis is a method for analytically determining the load-settlement relationship of a single pile based on the pile tip resistance-tip settlement relationship and the shaft resistance-settlement relationship of the pile obtained from previous loading test results. Specifically, as shown in Fig. 9, the pile body is assumed to be elastic and divided into several pile elements, and the analytical model considers friction springs along the pile shaft and an axial vertical spring at the pile tip. The hyperbolic curves expressed in Equations [10] and [11] are used to represent the friction spring between the pile shaft and the surrounding soil and an axial spring between the pile tip and the ground below.

$$q_p = S_p/\left(a_p + b_p S_p\right) \quad [10]$$

$$f_i = S_i/\left(a_f + b_f S_i\right) \quad [11]$$

$a_p$, $b_p$, $a_f$ and $b_f$ are the respective coefficients, the reciprocals $1/a_p$ and $1/a_f$ of which are the initial tangential slopes of the respective hyperbolic curves, and the reciprocals $1/b_p$ and $1/b_f$ are the asymptotic values (see Fig. 10). The coefficients $a_p$, $b_p$, $a_f$ and $b_f$ are obtained using regression lines with the $N$ values for each soil type obtained from numerous loading test results of the pre-boring method (Table 3).

The regression lines with the $N$ values for the coefficients $a_p$, $b_p$, $a_f$ and $b_f$ are given in reference (Ito A., 2008). The respective coefficients were calculated from the excavation diameter and excavation cross section. Therefore, the compressive deformation of the pile body was evaluated assuming that the entire excavation diameter, including the cement grout and the pile body. The modulus of elasticity, $E_p$, of the uniformly elastic body is obtained from Equation [12]. The modulus of elasticity of the pile body and cement grout were adopted as typical values of $E_c$=40000 N/mm$^2$ and $E_m$=4000 N/mm$^2$, respectively. $A_c$ is the cross-sectional area of the pile shaft section and $A_m$ is the cross-sectional area of the cement grout section.

 

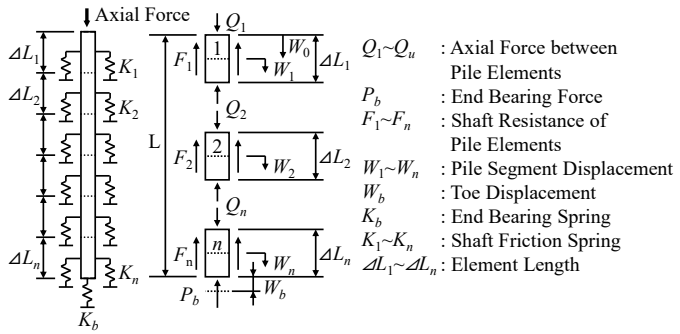


**Fig. 9. Load Transfer analysis model**

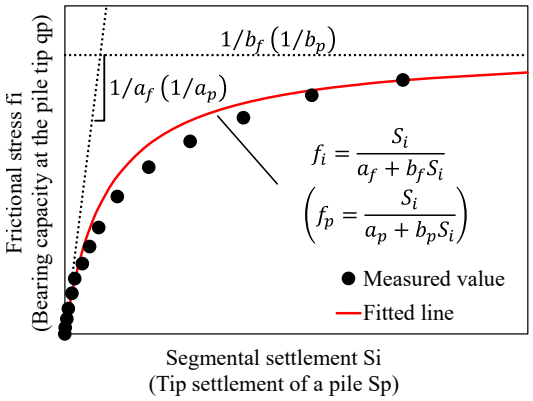


**Fig. 10. Overview of hyperbolic approximation**

**Table 3. Regression line of hyperbolic constant**

**(a) $q_p$-$S_p$ Curve**

| Soil | Constant | Regression equation |
|---|---|---|
| Sand | $1/a_p$ | 18200$N$+13700 |
| | $1/b_p$ | 243$N$+49.4 |
| Clay | $1/a_p$ | 12400$N$+67500 |
| | $1/b_p$ | 38.0$N$+1000 |

**(b) $f_i$-$S_i$ Curve**

| Soil | Constant | Regression equation |
|---|---|---|
| Sand | $1/a_f$ | 1580$N$+10900 |
| | $1/b_f$ | 243$N$+67.1 |
| Clay | $1/a_f$ | 1750$N$+15000 |
| | $1/b_f$ | 4.40$N$+50.1 |

$$E_p = (E_c A_c + E_m A_m)/(A_c + A_m) \quad [12]$$

***Results of verification***

Fig. 11 shows the comparison of pile head load-settlement relationships and Table 4 shows the comparison of pile head settlement at each design load (Long-term, Short-term, and Ultimate). It can be seen that the load transfer analysis was able to reproduce the load-settlement relationships of the piles obtained from the loading tests. The measured/analytical values of the pile head settlement at each design load range from 0.78 to 1.72. Fig. 12 shows the comparison results of axial force distribution (Long-term, Short-term, and Ultimate). The load transfer analysis successfully reproduces the pile's axial force distribution as observed in the loading test. While a discrepancy exists between the measured and analyzed values at ultimate load, this analytical accuracy is deemed sufficient when considering the inherent uncertainties of the ground.

 

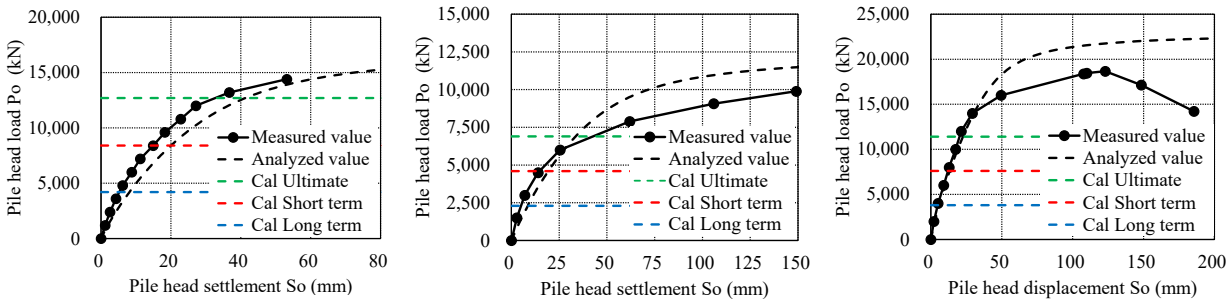


(a) Case 1 (b) Case 2 (c) Case 3

**Fig. 11. Pile Head Load-Settlement Relationship**

**Table 4. Comparison Measured Values and Analyzed Values (pile head settlement $S_o$(mm))**

| Test Case | Case 1 | | | Case 2 | | | Case 3 | | |
|---|---|---|---|---|---|---|---|---|---|
| State | Long term | Short term | Ultimate | Long term | Short term | Ultimate | Long term | Short term | Ultimate |
| Measured Values | 5.2 | 14.9 | 32.7 | 5.0 | 14.7 | 42.8 | 4.8 | 12.1 | 20.2 |
| Calculate Values | 8.1 | 19.8 | 39.5 | 8.6 | 19.3 | 33.5 | 5.8 | 13.3 | 22.4 |
| Measured/Calculated | 1.55 | 1.32 | 1.21 | 1.72 | 1.31 | 0.78 | 1.21 | 1.09 | 1.11 |

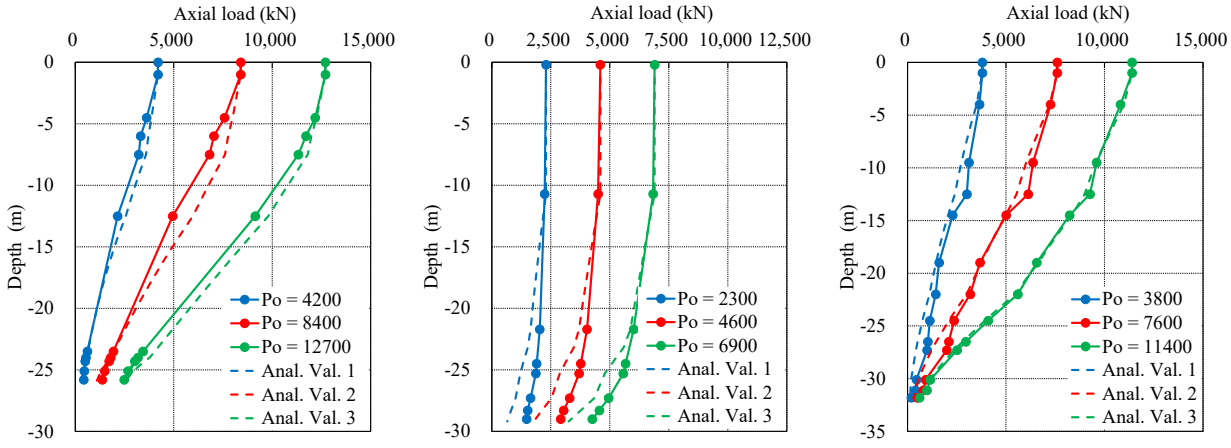


(a) Cace 1 (b) Case 2 (c) Case 3

**Fig. 12. Axial distribution curves**

## CONCLUSION

In this paper, an overview of the HM method and its bearing capacity evaluation equation are described, and the measured and calculated load bearing and load transfer mechanisms of the HM method are compared. The results showed that the load transfer analysis effectively replicates the pile's load-settlement characteristics and axial force distribution derived from the loading test results. Continuing with further load testing on fully instrumented piles will help expand the dataset and contribute to improved reliability

 

of the design approached developed for specific installation methods and pile types.

**REFERENCES**

Toyoshima, M.: Special Course on Foundations by Illustrations, Building Material Research Association, 1975 (in Japanese).

Ogura, H. Komatsu, G. Manabe, M. Oshima, A. Chikusa, N. Hosoda, Y. Sumi, M. and Mimura, T.: Enlarged Boring Diameter and Vertical bearing Capacity Installed by Root Enlarged and Solidified Pre-boring Method of Precast Pile, GBRC, Vo.32, No.1, pp.10-21, 2007 (in Japanese).

Japanese Society of Soil Mechanics and Foundation Engineering: Design and Explanation of Pile Foundations, Chapter 5 Calculation of Axial Bearing Capacity of Piles, 1985 (in Japanese).

Ito A., Ogura H., Tanaka Y. and Han H.: Estimation of Load-Settlement Relations on Pre-boring Nodular Piles, J. Struct. Constr. Eng., AIJ, No. 628, pp.907-913, Jun.,2008 (in Japanese).

Architectural Institute of Japan: Recommendation for Design of Building Foundation, pp.222-224, 2019.11 (in Japanese).

 